

# A MODEL FOR ULTRAFAST CHEMICAL DYNAMICS.

**E.I. Kats (L.D.Landau Institute, Moscow;  
Laue-Langevin Institute, Grenoble)**

*In the collaboration with:*

*V.A.Benderskii, E.V.Vetoshkin,*

*H.P. Trommsdorff.*

*Chem. Phys. Lett., v. 409, p.240 (2005).*

**Photochromism is a reversible transformation in a chemical species between two forms having different absorption spectra by photoirradiation. It is of special interest for optical data memory systems (photon mode erasable optical recording media). Examples: single molecules; polymers, biological molecules , e.g., photoisomerization of retinal in bacteriorhodospin. Advantages: speed of writing, fatigue due to material movement is eliminated. Requirements: high quantum yields and fast and non destructive read-out and write capability.**

**The chemistry of life requires a myriad of various reactions. All these reactions proceed with remarkable efficiency, speed and selectivity.**

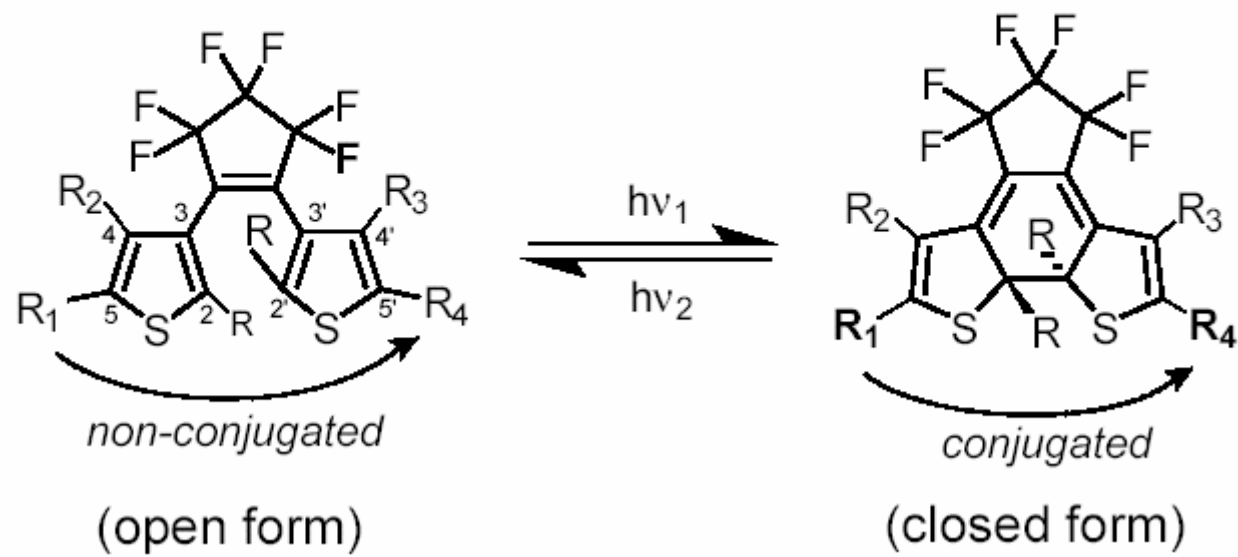
**Many important chemical transformations proceed on the femtosecond time scale. Methods to investigate: Pump-probe techniques, where an ultrashort pulse excites a chromophore and triggers the process to be investigated.**

**The attempt to get information from On or Off states results to undesirable change of information: the switch state is altered by the action of the reading method. A solution to this problem: molecules which present not only absorption bands active to the opening closing procedure but also present additional bands inactive to the switching action. Reading could be easily effected by the irradiation of these inactive bands. These systems are photoswitchable molecular wires.**

**The primary event that initiates vision is the light induced cis-trans isomerization of retinal in the visual pigment rhodospin. It is the fastest photochemical reaction in nature and is complete in only 200 fs with quantum yield 0.6.**

**Dissipation of molecular vibrational excitation energy typically takes place on ps scale. So molecules must be able to channel energy more rapidly to direct it in a useful manner.**

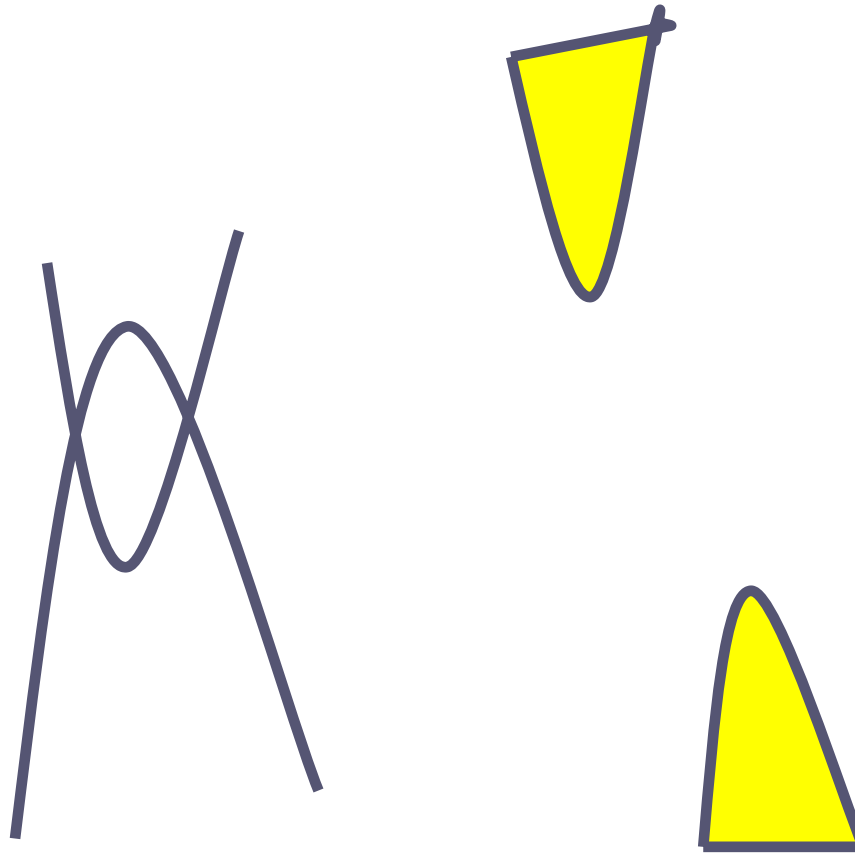
The bis -thien -3 -yl perfluorocyclopenten:



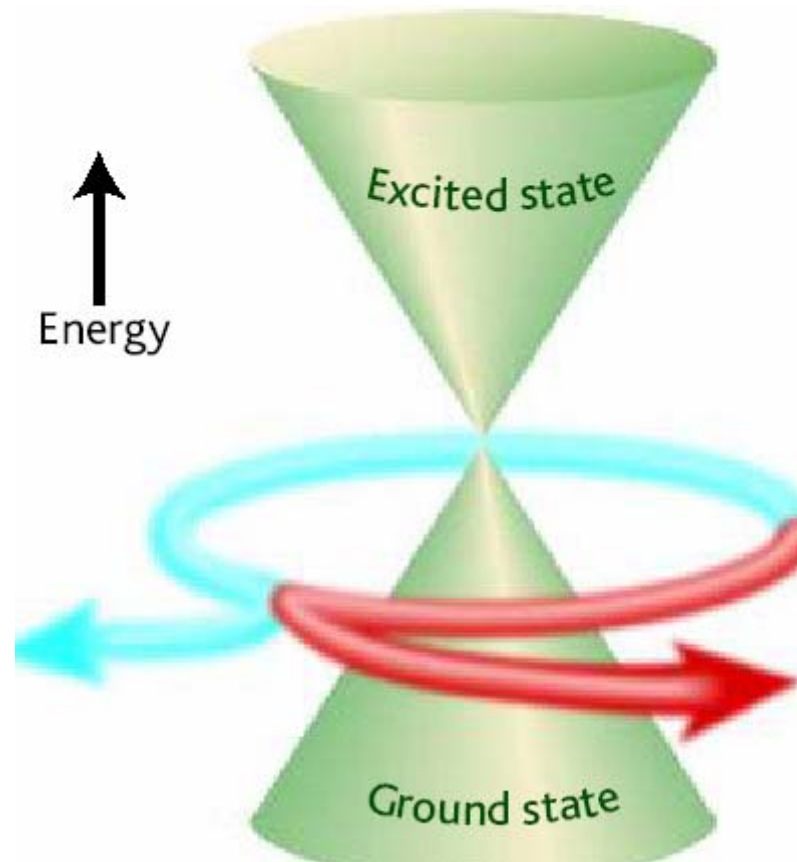
**To understand chemical reactions, theorists solve the Schrodinger equation for electrons to calculate potential energy surfaces on which the nuclei move. These surfaces are then used in quantum dynamical computations that solve the Schrodinger equation for the nuclei taking part in the reaction at different energies.**

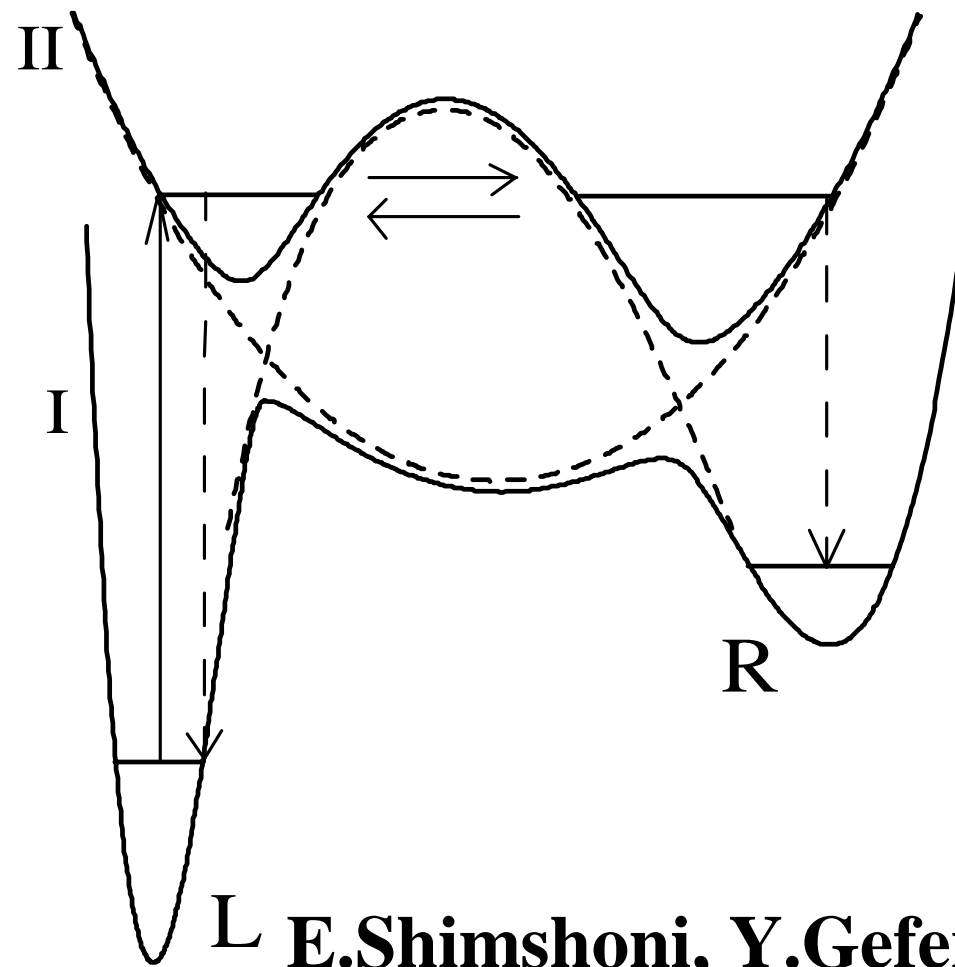
**The predominant reaction pathway is often summarized in the form of a simple potential energy.**

# L.Salem, Science (1976).

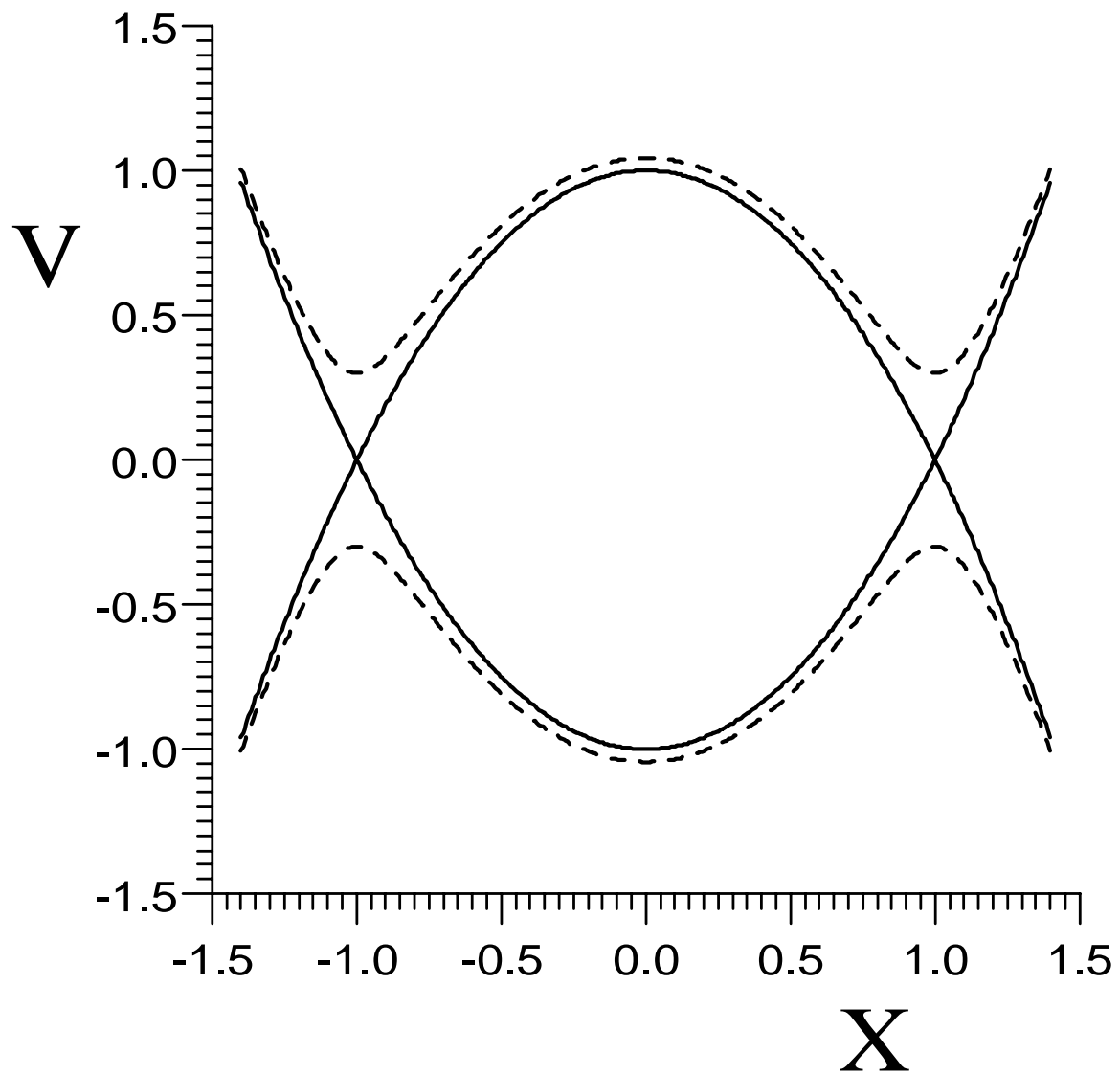


PES, describing each of the two isomers. Efficient and ultrafast conversion occurs when the splitting of these PES at the avoided crossing is not too large. For a large gap, isomerization occurs only subsequent to vibrational relaxation and will not be ultrafast. The case of a lower energy excited state PES, intersecting twice the ground state barrier was discarded, since the resulting adiabatic upper PES has two minima, separated by a barrier, and slow tunneling through this barrier was thought to limit the reaction rate.





**L E. Shimshoni, Y. Gefen  
Ann. Phys. (1991).**

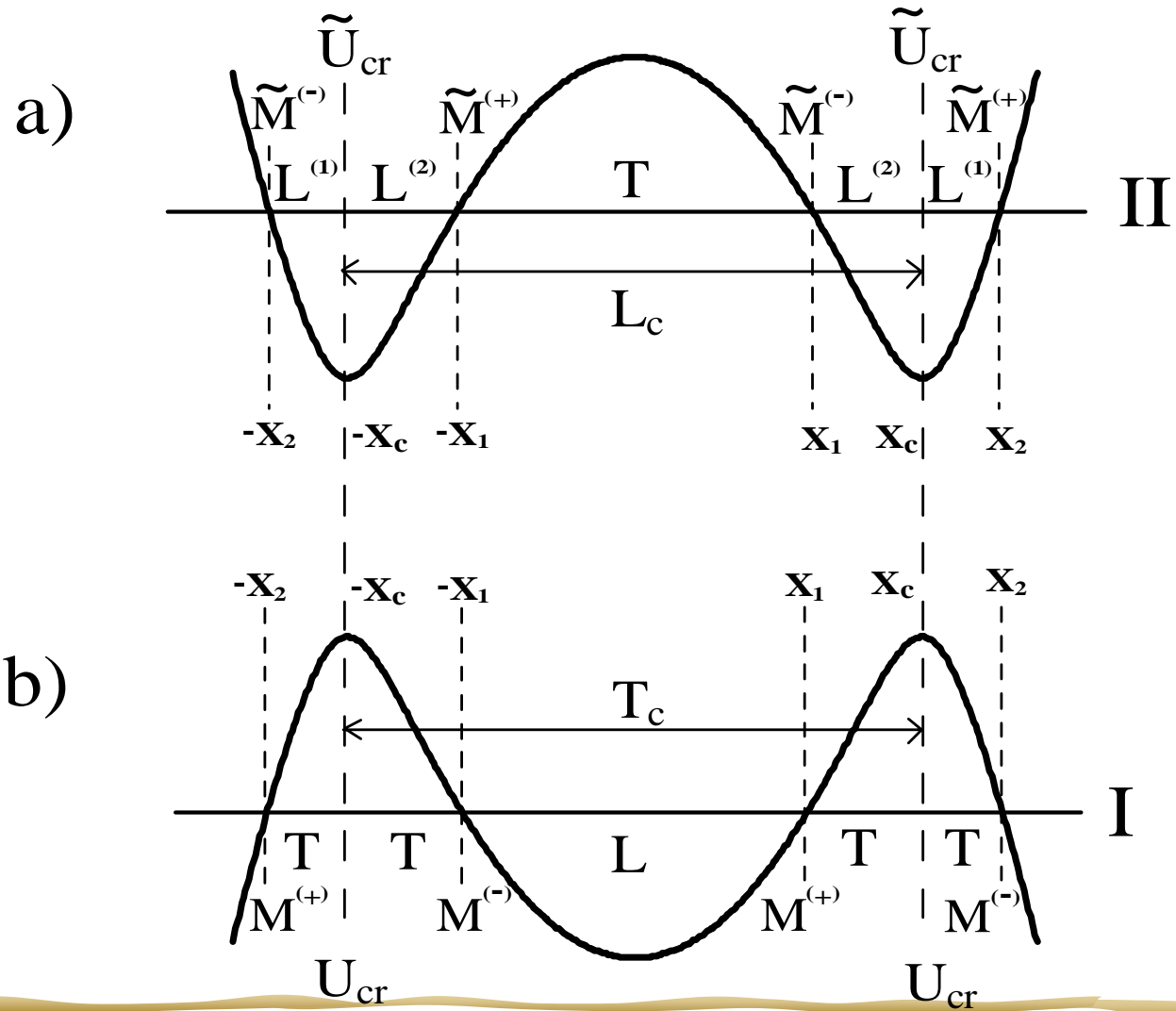


$$V = \begin{pmatrix} -a + (X + X_0)^2 & u_{12} \\ u_{12} & a - (X - X_0)^2 \end{pmatrix}$$

$$\gamma = \frac{m\Omega a^2}{\hbar}$$

**Connection matrices match asymptotically semiclassical (approximate) solutions for the exact (model) potential to the exact solutions with approximate near stationary points potentials (comparison equations: Airy and Weber functions.**

**Full connection matrix is a matrix product of the elementary connection matrices at stationary points and diagonal shift matrices translating solutions between the stationary points (depending on the actions: Imaginary in classically forbidden regions and real in classically accessible regions.**



$$V^{\pm}(X) = \pm \sqrt{(1 - X^2)^2 + u_{12}^2}.$$

$$-\sqrt{1 + u_{12}^2} = \min V^- < \frac{\varepsilon}{\gamma} < \max V^- = -u_{12},$$

$$\hat{U} = \hat{M} \begin{pmatrix} \hat{L} & 0 \\ 0 & \hat{T}_c \end{pmatrix} \hat{M},$$

$$\hat{M} = \begin{pmatrix} \hat{M}^{(-)} \hat{T} & 0 \\ 0 & 1 \end{pmatrix} \hat{U}_c \begin{pmatrix} \hat{T} \hat{M}^{(+)} & 0 \\ 0 & \hat{T}_c \end{pmatrix}.$$

$$\hat{L} = \begin{pmatrix} \exp(i\gamma W_0) & 0 \\ 0 & \exp(-i\gamma W_0) \end{pmatrix},$$

$$W_0 = \int_{-X_1}^{X_1} dX \sqrt{2 \left( \frac{\varepsilon}{\gamma} - V^- \right)}.$$

$$\hat{T}_c = \begin{pmatrix} \exp(\gamma W_c) & 0 \\ 0 & \exp(-\gamma W_c) \end{pmatrix},$$

$$W_c = \int_{-X_c}^{X_c} dX \sqrt{2 \left( V + - \frac{\varepsilon}{\gamma} \right)}.$$

$$\hat{T} = \begin{pmatrix} \exp(-\gamma W_b/2) & 0 \\ 0 & \exp(\gamma W_b/2) \end{pmatrix},$$

$$\nu \equiv u_{12}^2 / (4\sqrt{\varepsilon})$$

**Massey parameter**

$$W_b = \int_{X_1}^{X_2} dX \sqrt{2 \left( V - \frac{\varepsilon}{\gamma} \right)}.$$

$$\hat{U}_c = \begin{bmatrix} p & 0 & 0 & -\cos(\pi\nu) \\ 0 & (\sin^2(\pi\nu))/p & -\cos(\pi\nu) & 0 \\ 0 & \cos(\pi\nu) & p & 0 \\ \cos(\pi\nu) & 0 & 0 & (\sin^2(\pi\nu))/p \end{bmatrix}$$

$$p = \frac{\sqrt{2\pi} \exp(-2\chi)}{\Gamma(\nu)},$$

$$\chi = (\nu/2) - (1/2) (\nu - (1/2)) \ln \nu.$$

$$\begin{pmatrix} A_R \\ B_R \\ C_R \\ D_R \end{pmatrix} = \hat{U} \begin{pmatrix} B_L \\ A_L \\ D_L \\ C_L \end{pmatrix}.$$

$$A_R = A_L = C_R = C_L = 0,$$

$$U_{22}U_{33} - U_{23}U_{32} = 0,$$

**C – exponentially increasing solutions for the upper potential adiabatic potential;**  
**D – exponentially decreasing solutions for the upper adiabatic potential;**  
**A – ingoing waves and B – outgoing waves for the lower adiabatic potential.**

$$Aq^2 + Bq + C = 0,$$

$$q \equiv \cot u, \quad u \equiv \gamma W_L - \phi, \quad W_L \equiv W_L^{(1)} + W_L^{(2)}$$

$$A = s^2 - \frac{1}{2}s^2(1 - s^2) \exp(-b) \exp(iw) + \frac{1}{2}(1 - s^2)^2 \exp(iw) \cos w,$$

$$B = -i(1 - s^2)[s^2 + (1 - s^2) \exp(iw) \cos w],$$

$$C = -\frac{1}{4} \exp(-2b) - \frac{1}{2}s^2(1 - s^2) \exp(-b) \exp(iw) - \frac{1}{2}(1 - s^2)^2 \exp(iw) \cos w,$$

$$s = \sqrt{1 - \exp(-2\pi\nu)}, \quad w \equiv 2\gamma W_L^{(1)} + \gamma W_c; \quad b \equiv \gamma W_b.$$

$$\phi = -\arg \Gamma(-i\nu);$$

$$2\pi\nu > \gamma W_b$$

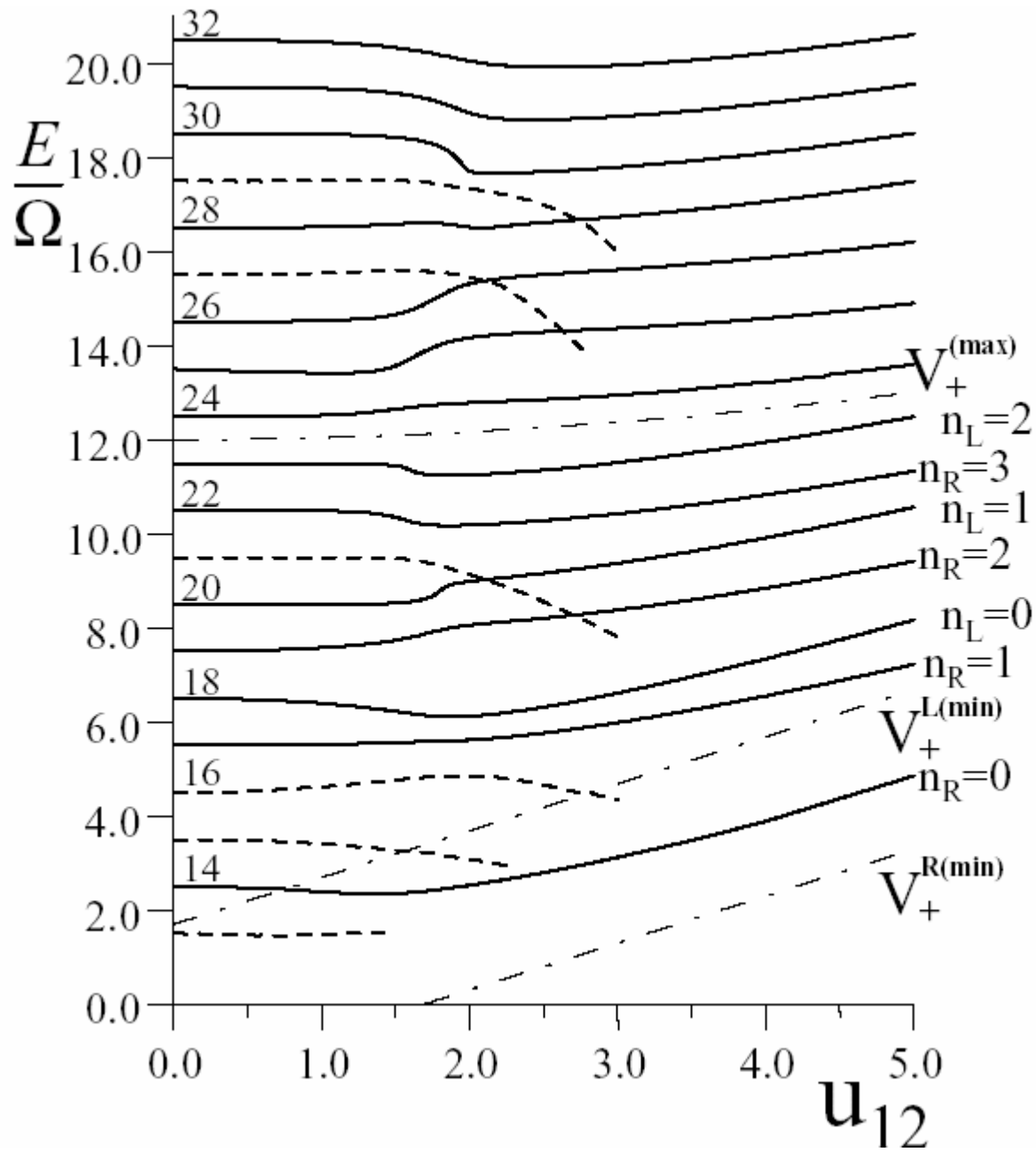
$$\epsilon_n^{(0)} \simeq \omega(\epsilon_n^{(0)}) \left[ n + \frac{1}{2} \pm \frac{1}{2\pi} \exp(-b) \right]$$

$$\epsilon_n^{(0)} \simeq \omega(\epsilon_n^{(0)}) \left[ n + \frac{1}{2} \pm \frac{1}{2\pi} (1 - s^2) \cos w \right],$$

$$\Gamma_n \simeq \frac{\omega(\epsilon_n^{(0)})}{\pi} (1 - s^2) (2 - s^2 \pm \sin w).$$

$$\epsilon_{n'}^{(0)} \simeq \omega(\epsilon_{n'}^{(0)}) \left[ n' + \frac{1}{2} - \frac{s^2}{2\pi} (\sin(2u) + (-1)^{n'} \exp(-b) \cos(2u)) \right],$$

$$\Gamma_{n'} \simeq 2 \frac{\omega(\epsilon_{n'}^{(0)})}{\pi} s^2 (2 \cos^2 u - (-1)^{n'} \exp(-b) \sin(2u)).$$



Real parts of the eigenvalues as functions of adiabatic coupling strength,  $u_{I2}$ , in a potential with  $X_0 = 0.1$ , and  $\gamma = 12$ . Quantum numbers,  $n'$ , of the harmonic diabatic potential are indicated (for clarity only even numbers) at the left, while on the right side those of  $Q_R$ - and  $Q_L$ -states of the upper adiabatic potential are shown. D-states are marked by dashed lines up to values of  $u_{I2}$ , for which the imaginary part of eigenvalues exceeds the energy spacings. The evolution of the stationary points,  $V_+^{L(\min)}$ ,  $V_+^{R(\min)}$ ,  $V_+^{(\max)}$ , of the upper adiabatic potential are shown by dash-dotted lines.

**Bold lines:**

**Q-states (non-monotonic decay);**

**Dashed lines :**

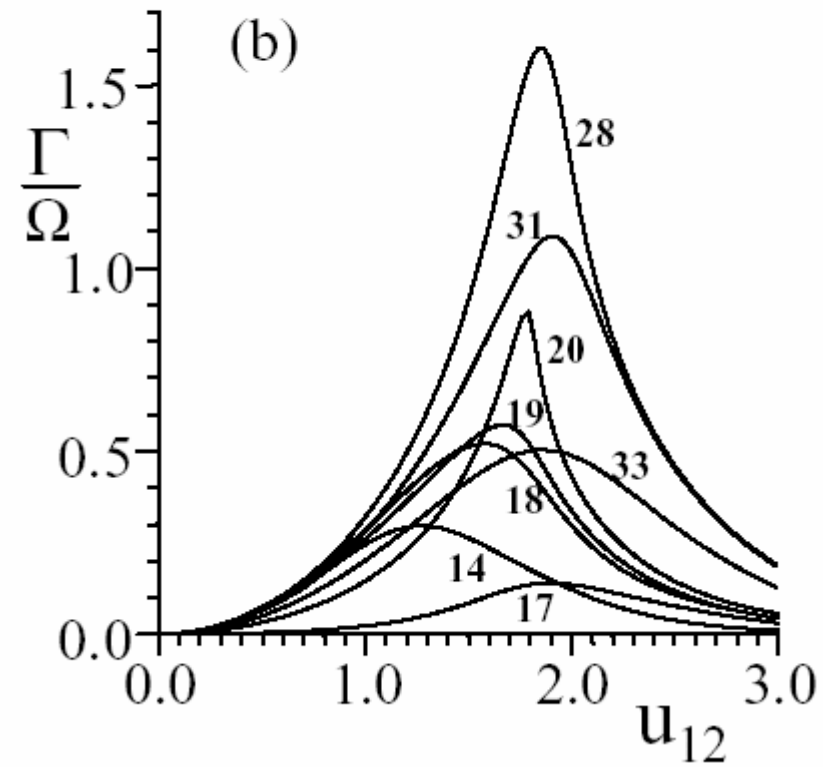
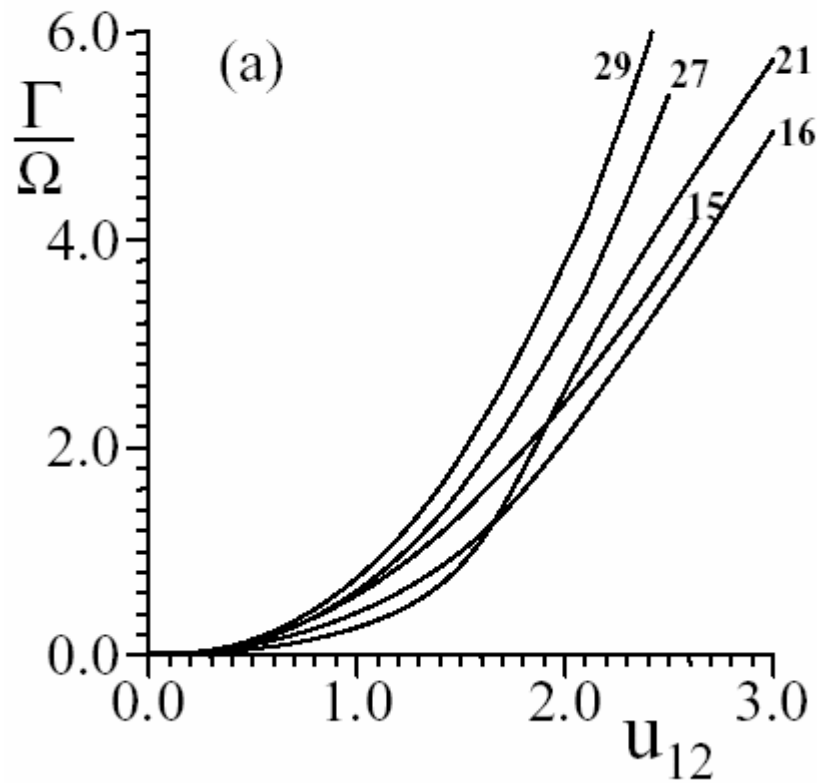
**D-states (monotonic decay);**

**Dot-dashed lines:**

**Maximum and minima of the upper adiabatic potential.**

**Left numbers – diabatic quantum numbers;**

**Right numbers – adiabatic quantum numbers.**



$$u_{12} = \min V^+ < \frac{\varepsilon}{\gamma} < \max V^+ = \sqrt{1 + u_{12}^2},$$

$$\hat{U}_c = \begin{bmatrix} s \exp(i\phi) & 0 & 0 & -\exp(-\pi\nu) \\ 0 & s \exp(i\phi) & -\exp(-\pi\nu) & 0 \\ 0 & \exp(-\pi\nu) & s \exp(-i\phi) & 0 \\ \exp(-\pi\nu) & 0 & 0 & s \exp(-i\phi) \end{bmatrix},$$

$$s = \sqrt{1 - \exp(-2\pi\nu)}, \quad \phi = \phi + \phi_0,$$

$$\phi = -\arg \Gamma(-i\nu); \quad \phi_0 = \nu(1 - \ln \nu) + \frac{\pi}{4}.$$

$$P \exp(i\gamma W_0) + Q \exp(-i\gamma W_0) + R = 0 ,$$

$$P = \frac{1}{4} \exp(-\gamma W_c) \cos(4\pi\nu) + \exp(\gamma W_c) \left[ \exp(\gamma W_b) - \frac{1}{4} p^2 \exp(-\gamma W_b) \right]^2 ,$$

$$Q = P + \frac{1}{2} p^2 \exp(\gamma(W_c - W_b)) ,$$

$$R = -\frac{1}{2} p^2 \exp(-2\gamma W_b) \cos^2(\pi\nu) .$$

$$\gamma W_0 = \pi \left( n + \frac{1}{2} \right) - (-1)^n \frac{Q}{\sqrt{PR}} + i \frac{P - R}{P + R} \quad \epsilon_n = \epsilon_n^{(0)} + i \frac{\Gamma_n}{2},$$

$$-\sqrt{1 + u_{12}^2} + \omega(\epsilon_n^{(0)}) \left[ n + \frac{1}{2} + \frac{p^2}{2\pi} \exp(-\gamma(W_c(\epsilon_n) + 2W_b(\epsilon_n))) \cos^2(\pi\nu) \right]$$

$$\Gamma_n = \omega(\epsilon_n^{(0)}) \frac{p^2}{\pi} \exp(-2\gamma W_b(\epsilon_n)).$$

$$\omega(\epsilon_n^{(0)}) \equiv \left( \frac{\partial \epsilon}{\partial W_0} \right)_{\epsilon = \epsilon_n^{(0)}}.$$

**Wave functions can be also calculated by the connection matrix technology.**

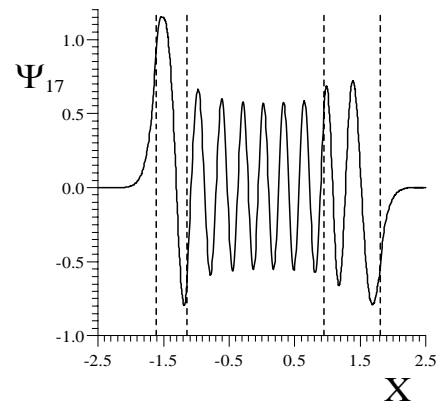
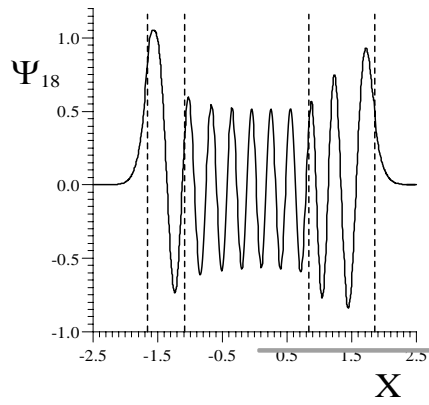
$$\Phi_n(X_k, X) = \hat{M}_k \hat{L}_{k,k-1} \hat{M}_{k-1} \dots \hat{M}_2 \hat{L}_{21} \hat{M}_1 \Phi_n(X, X_1),$$

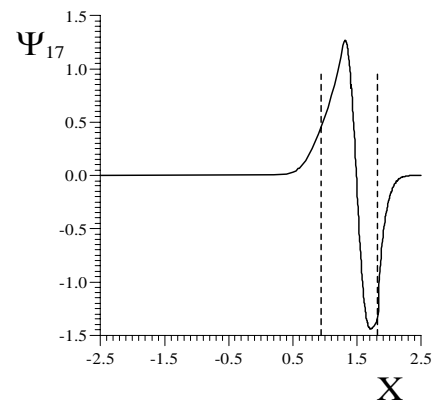
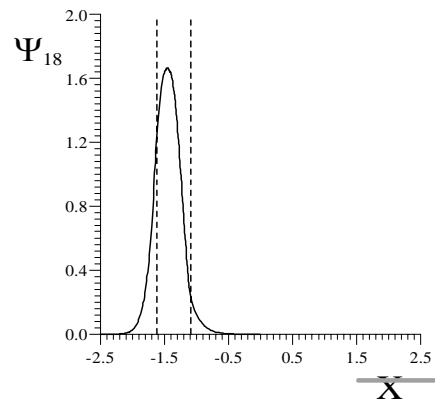
**Wave functions of the bound states for the upper adiabatic potential for the energy close to the ground state in the L-well.**

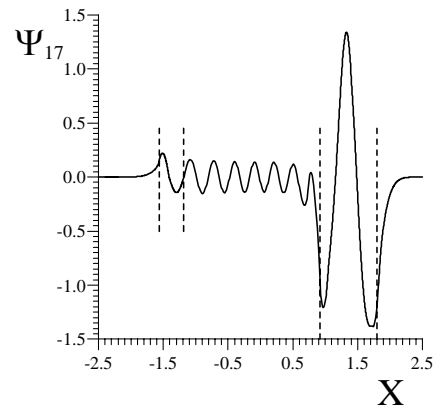
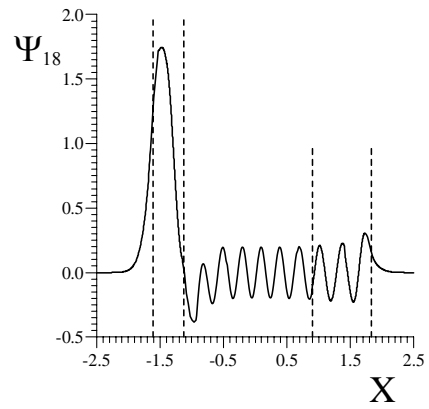
**In the diabatic limit the functions correspond to strongly excited states of the harmonic oscillator (extended in the broad region between the crossing points).**

**In the adiabatic limit the functions are localized within the wells of the upper adiabatic potential.**

**For the intermediate coupling strengths – the functions are combinations of localized and delocalized states.**







$$\Gamma_n^{R,L} = \left( \int |\Psi_n|^2 dX \right)^{-1} \left( \Psi_n \frac{d\Psi_n^*}{dX} - \Psi_n^* \frac{d\Psi_n}{dX} \right)_{X \rightarrow \pm\infty} .$$

$$Y_n^{L,R} = \frac{\Gamma_n^R}{\Gamma_n^R + \Gamma_n^L} .$$

$$\hat{V}(X) = \begin{pmatrix} -1 + (X + \delta)^2 & u_{12} \\ u_{12} & 1 - (X - \delta)^2 \end{pmatrix},$$

$$V^\pm(X) = 2\delta X \pm \sqrt{(\delta^2 + X^2)^2 + u_{12}^2}.$$

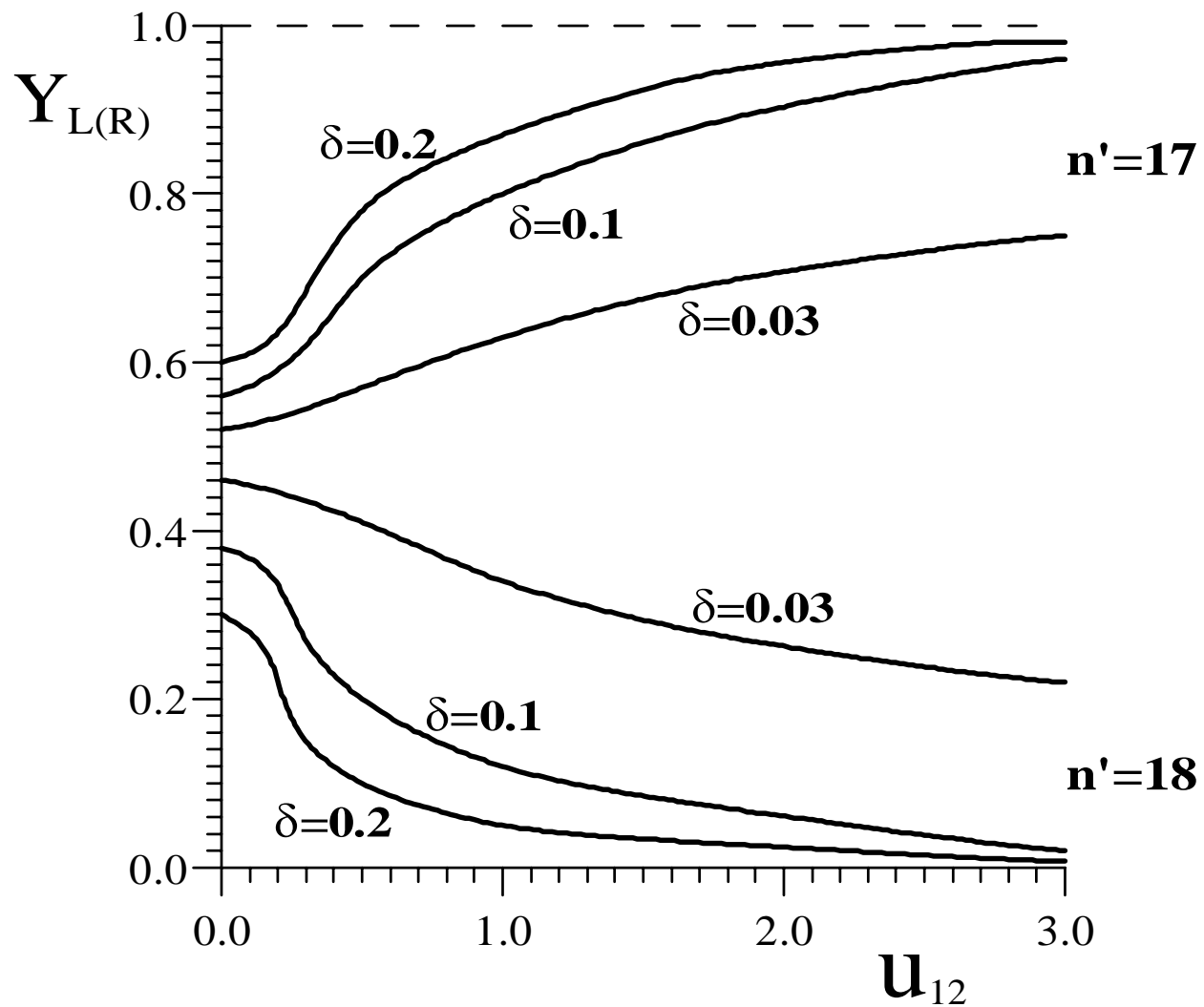
For a symmetric potential,  $X_0 = 0$ , this quantum yield always equals  $1/2$ . In the asymmetric potential, the quantum yield decreases as a function of  $u_{12}$  and reaches zero in the adiabatic limit due to the localization of adiabatic wave functions in the L or R wells. With increasing asymmetry, the region where  $Y_{LR}$  drops is shifted towards smaller values of  $u_{12}$ . However, in the intermediate region ( $u_{12} = 1-3$ ), high values of quantum yield ( $Y_{LR} \geq 0.1$ ) are preserved even when the asymmetry becomes comparable to the characteristic frequency. Moreover, for states above the barrier with  $E > 1.5 V^\ddagger$ ,  $Y_{LR} \approx 0.5$ . Our model, therefore, provides a basis for both experimental findings, namely the high quantum yield combined with ultrafast dynamics of photoisomerization reactions.

**In the diabatic limit:**

$$\left(1 + \frac{A}{u_{12}}\right)^{-1/2}$$

**In the adiabatic limit:**

$$[\Delta^2(n_L, n_R) + A^2(n_L, n_R)]^{+1/2}$$



**Decay rate should be averaged over environment spectrum. The effect is relevant in the adiabatic and diabatic limits but it is relatively small for the intermediate couplings.**

$$E = \epsilon_n + \rho(\tilde{\epsilon})\tilde{\epsilon}.$$

$$P(\Psi, t) \equiv |\langle \Psi(0) | \Psi(t) \rangle|^2 .$$

$$P(t) = \frac{1}{2} \exp(-\Gamma t) (1 \pm \cos(Et)) .$$

$$S(\Psi, E) = \sum_n |\langle \Psi | \Psi_n \rangle|^2 \delta(E - E_n)$$

$$P(t) = \int_{-\infty}^{+\infty} dE S(\Psi, E) \exp(iEt) .$$

Survival probability of the instantly prepared quasi-stationary state in the  $L$  well for the asymmetric potential:

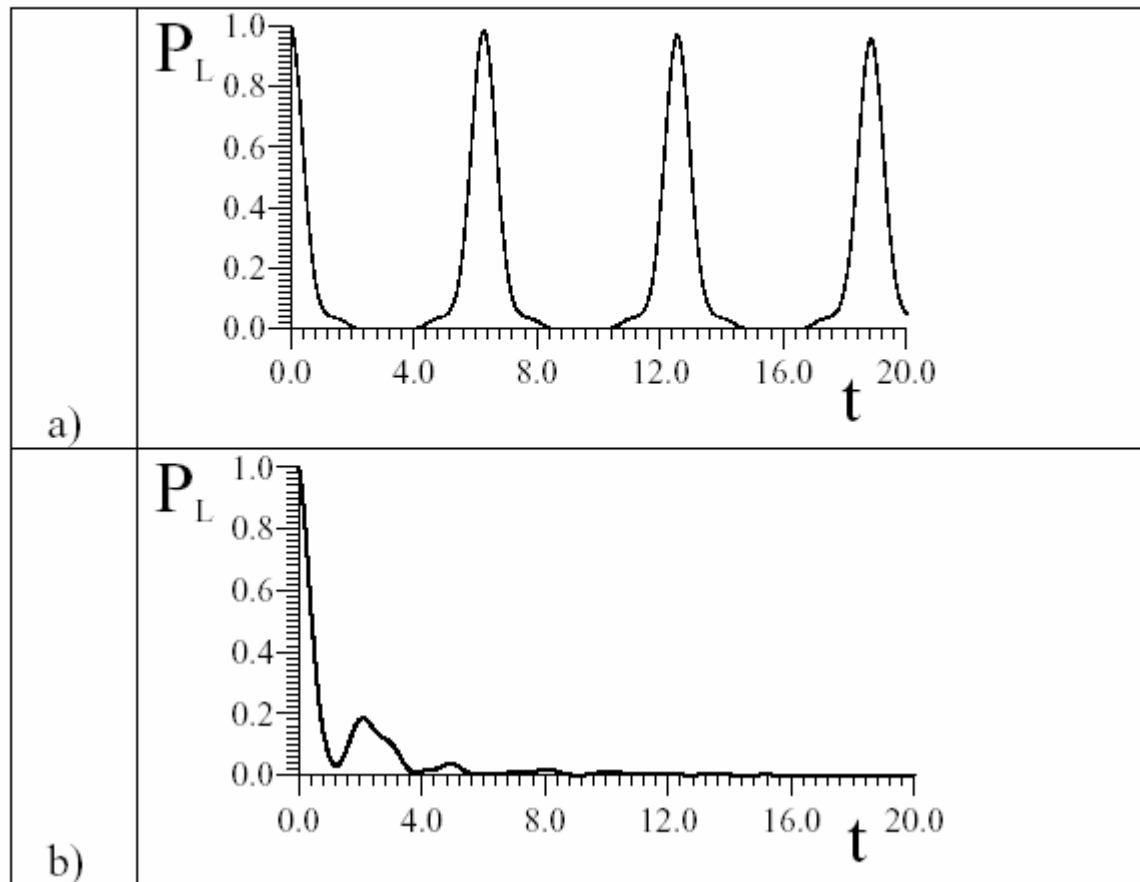
$\delta = 0.1$  , and  $\gamma = 12$  :

(a)  $u_{12} = 0.3$ ;

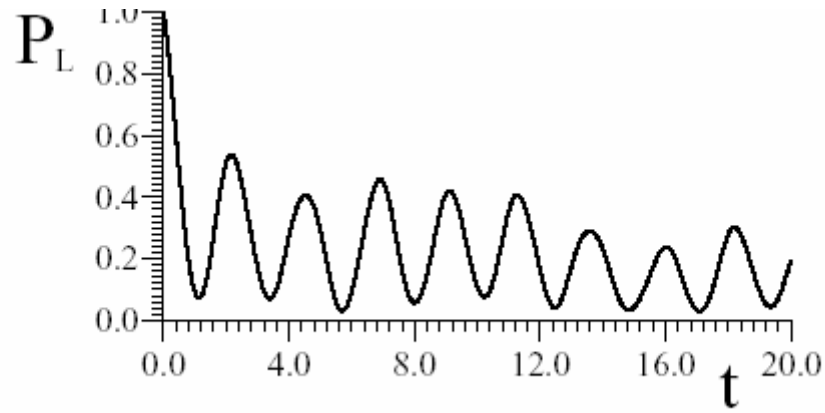
(b)  $u_{12} = 1.5$ ;

(c)  $u_{12} = 3.0$ ;

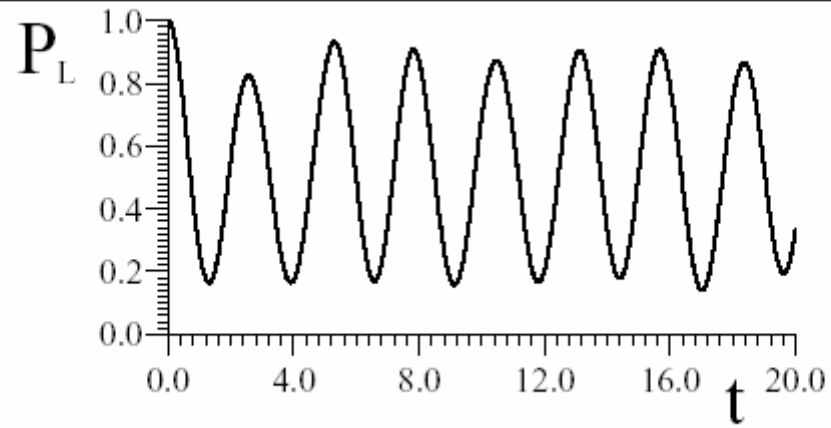
(d)  $u_{12} = 5.0$ .

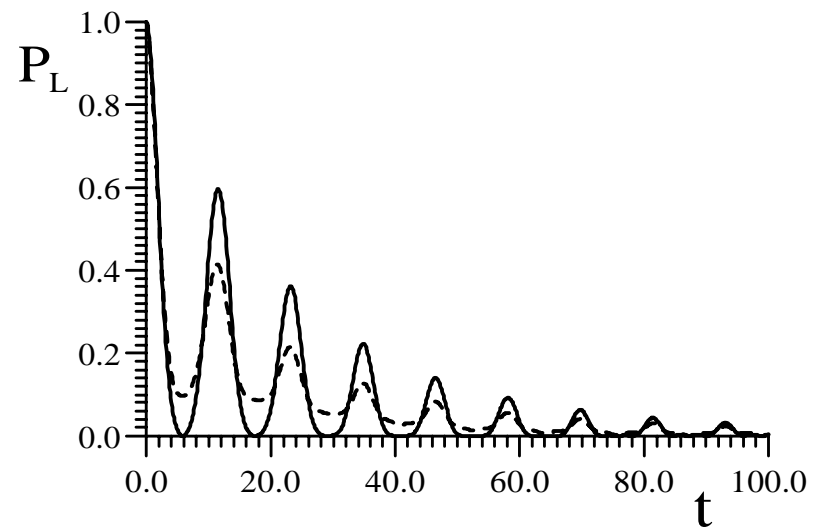
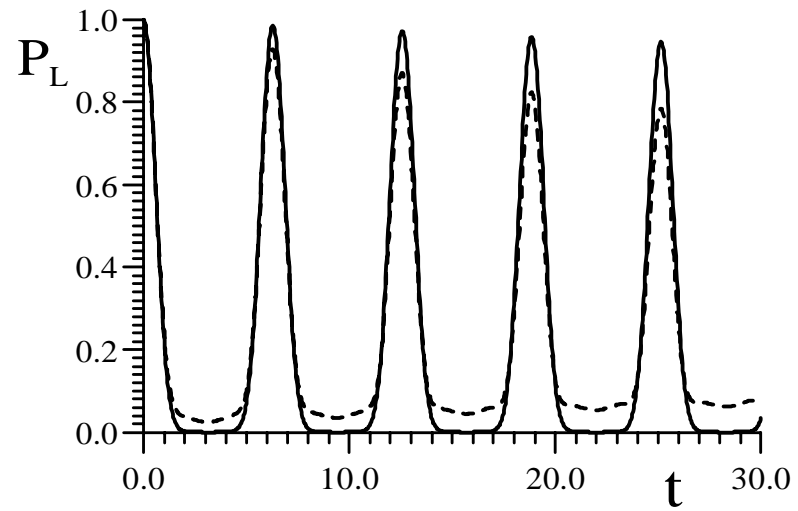


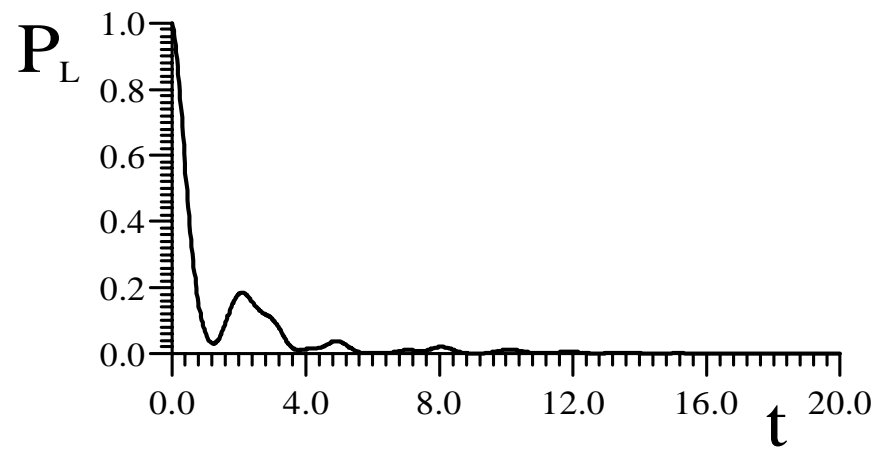
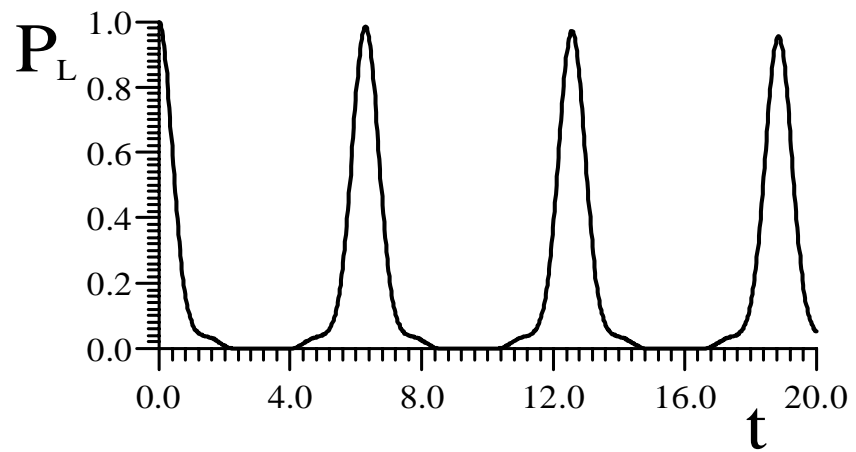
c)

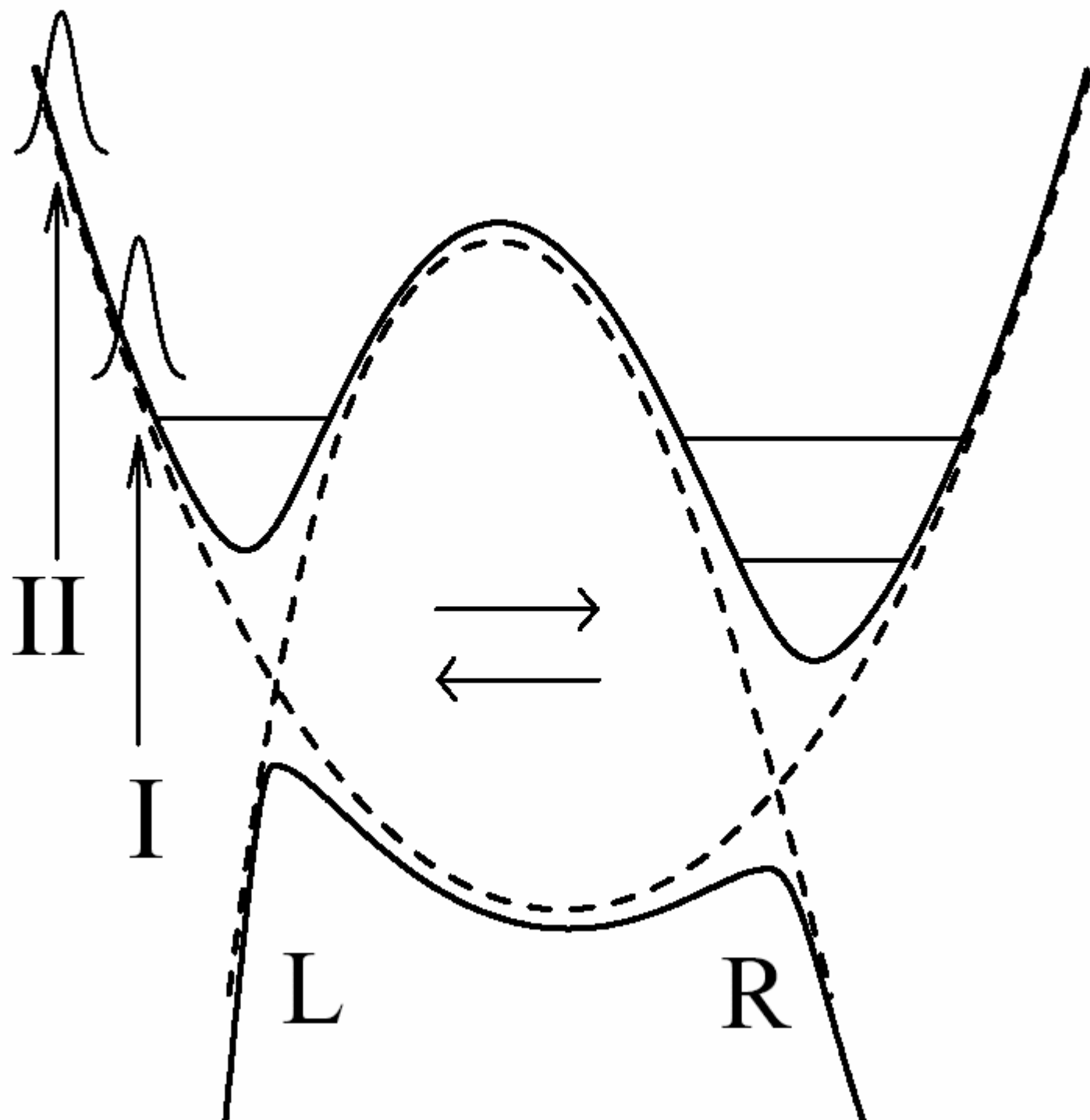


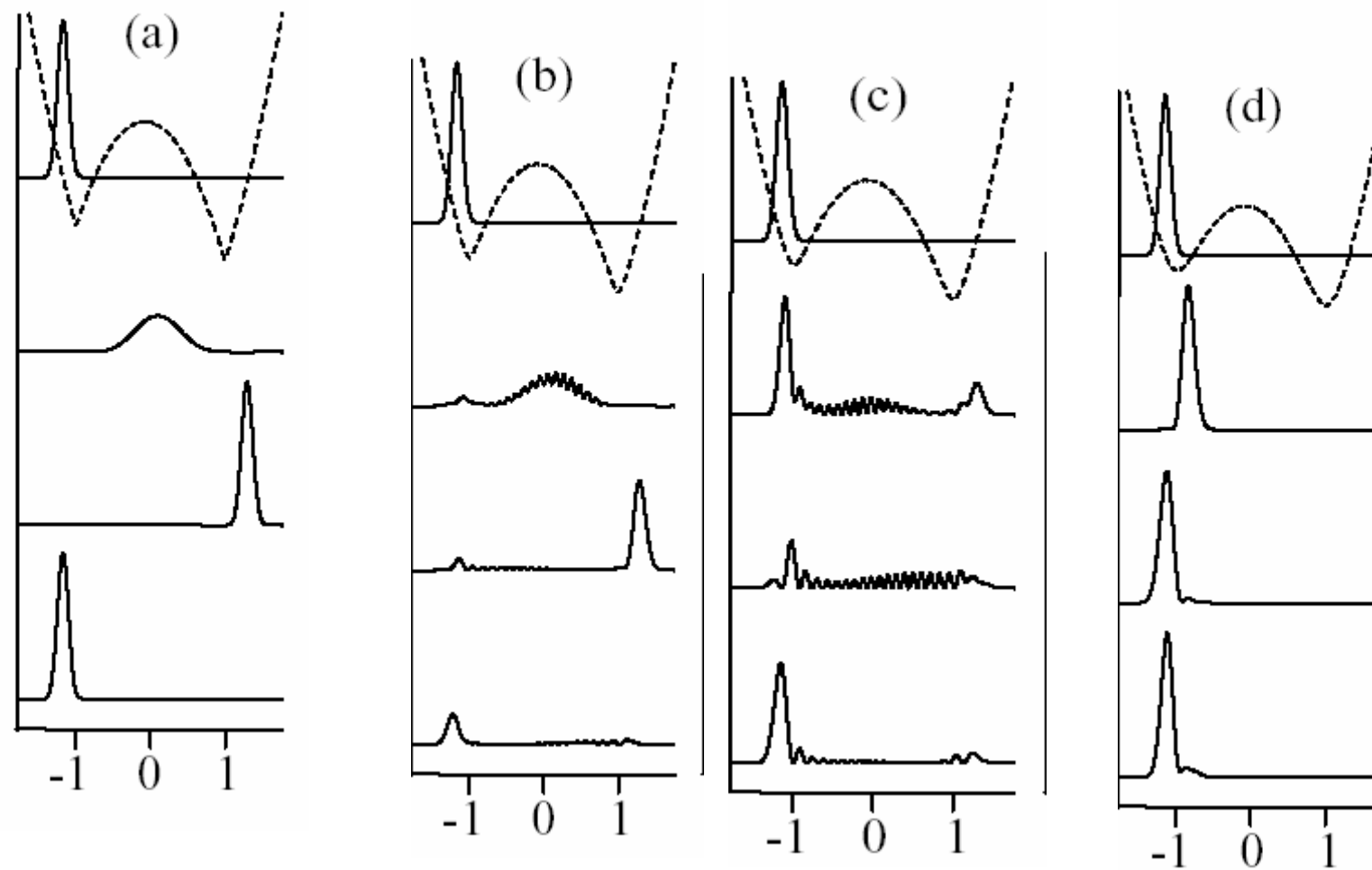
d)

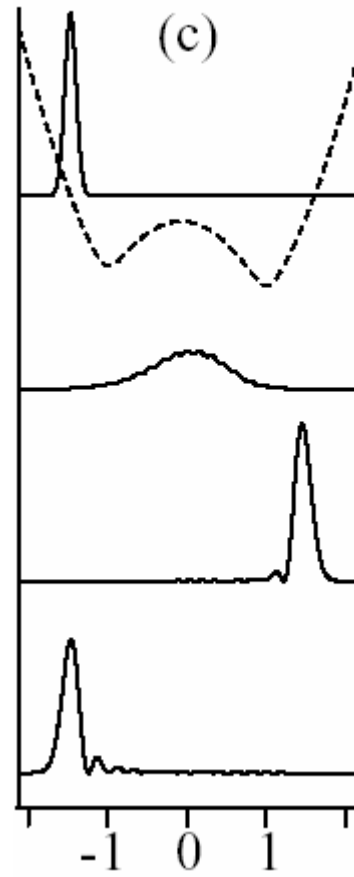
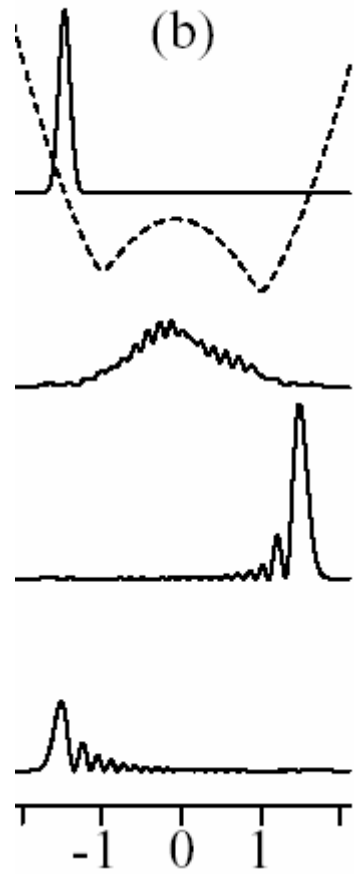
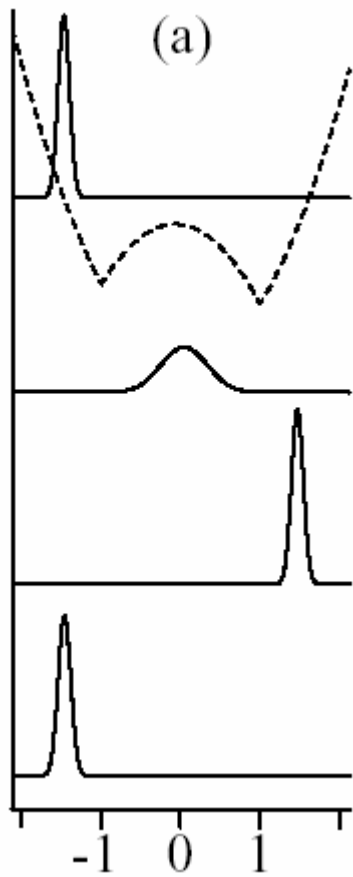












The time evolution of wave packets I and II has been calculated in the wide range of coupling constants from the diabatic ( $u_{12} = 0$ ) to the adiabatic ( $u_{12} \gg 1$ ) limit. The evolutions are shown in Figs. 4 and 5. In the diabatic limit, wave packet I spreads over the wide lower diabatic well and recovers near the turning points with the residual amplitude (Fig; 4a). As the coupling increases, the wave packet amplitude decreases due to the decay of Q-states (Fig. 4b, c). In the adiabatic limit (Fig. 4d), packet I is localized in the left well and its decay rate becomes small, since nonadiabatic transitions are suppressed. The behavior of wave packet II is similar to that of packet I not only in the diabatic limit, but also in the wide range of intermediate coupling (Fig. 5a, b). In contrast to packet I, packet II is delocalized in the adiabatic limit due to fast overbarrier transitions. The similarity of the dynamics of packets I and II in the wide intermediate range of coupling is the result of double nonadiabatic transitions.

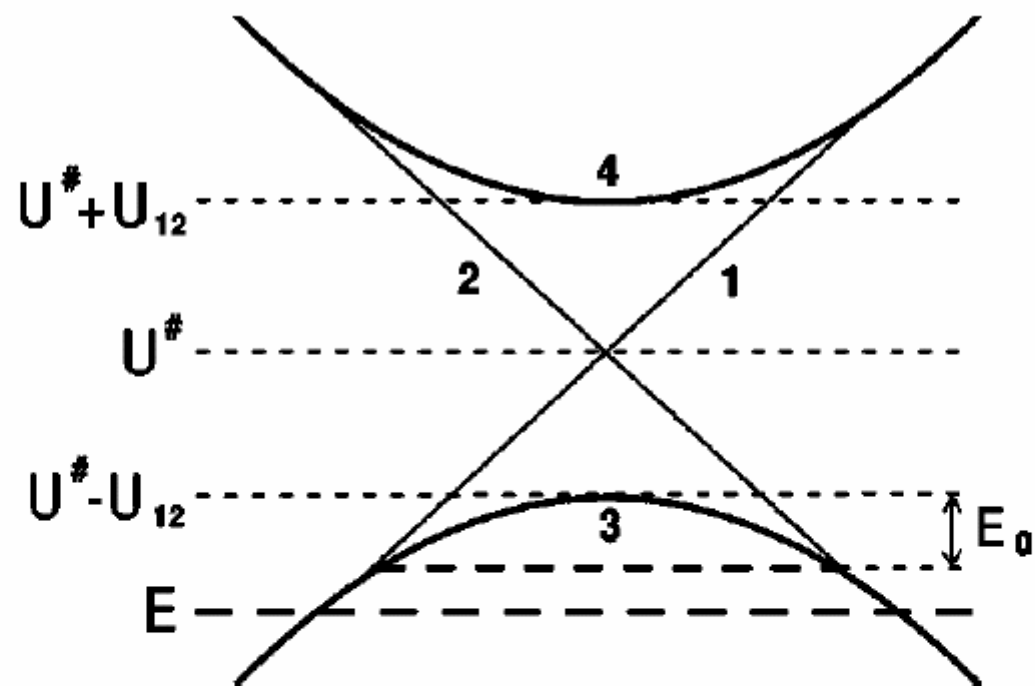
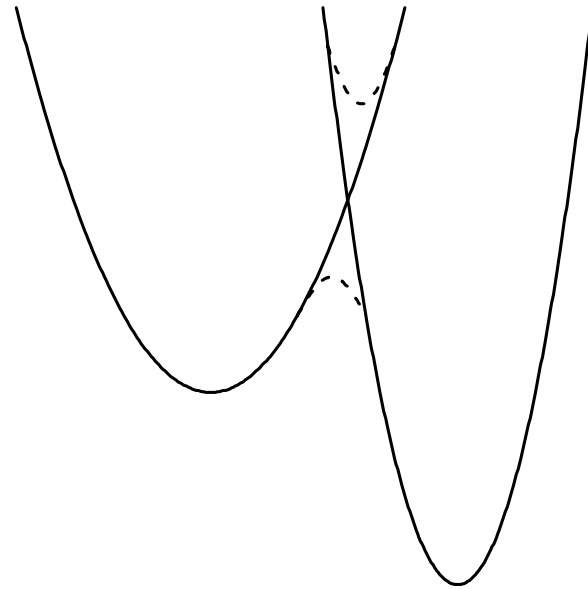
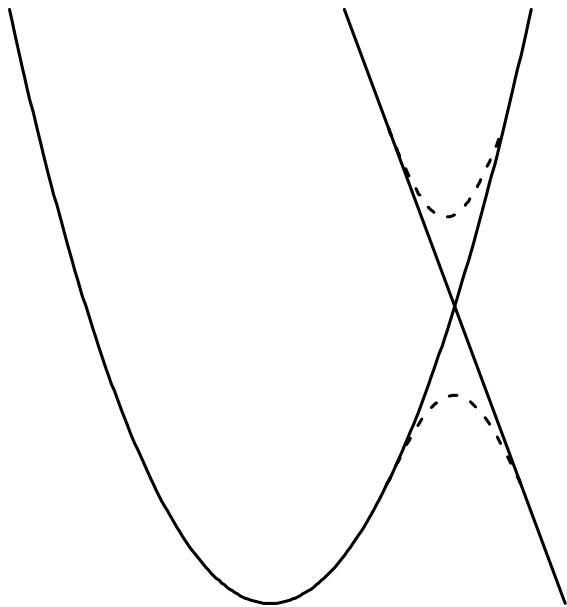
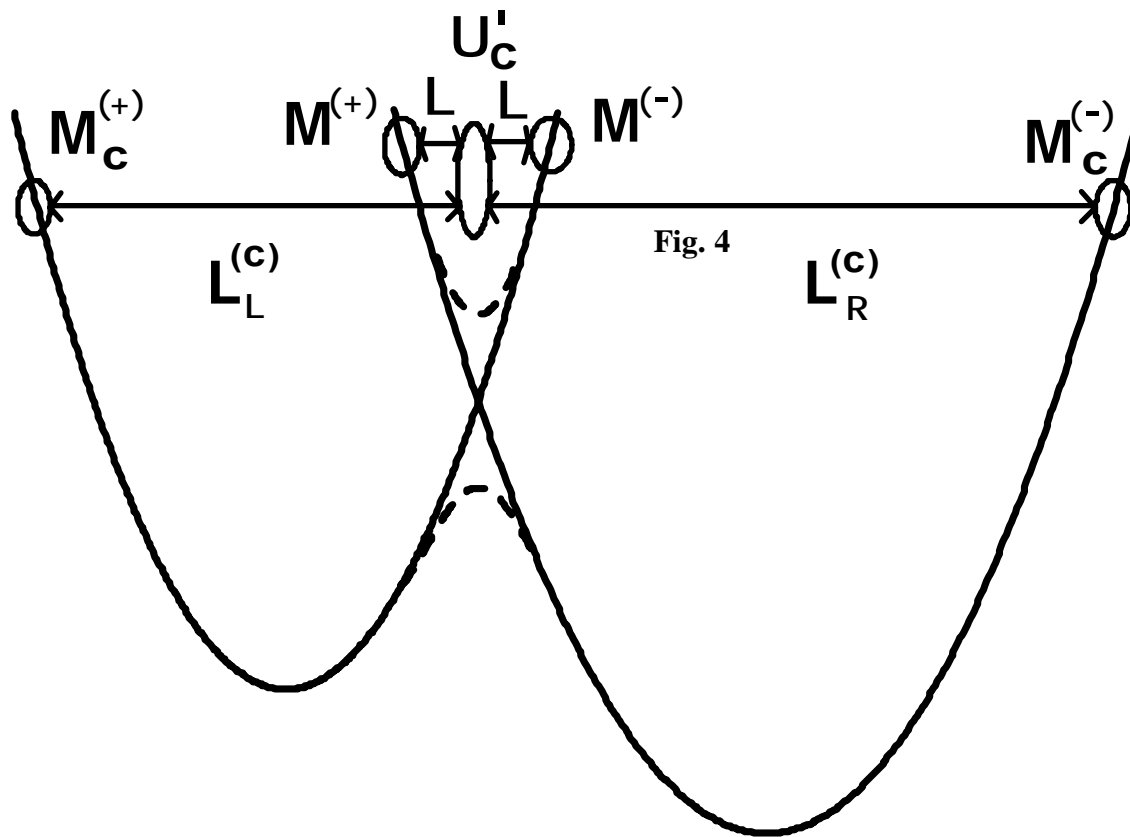


FIG. 1. Potentials in the vicinity of the diabatic potentials crossing point  $U^\#$ : The diabatic potentials (thin lines, 1,2), the adiabatic potentials (bold lines, 3,4), the adiabatic coupling energy  $U_{12}$ , and  $E_0$  is the characteristic zero-point oscillations energy in the parabolic barrier approximated the lower adiabatic potential near its top. The tunneling energy  $E$  region is shown by a broken line.





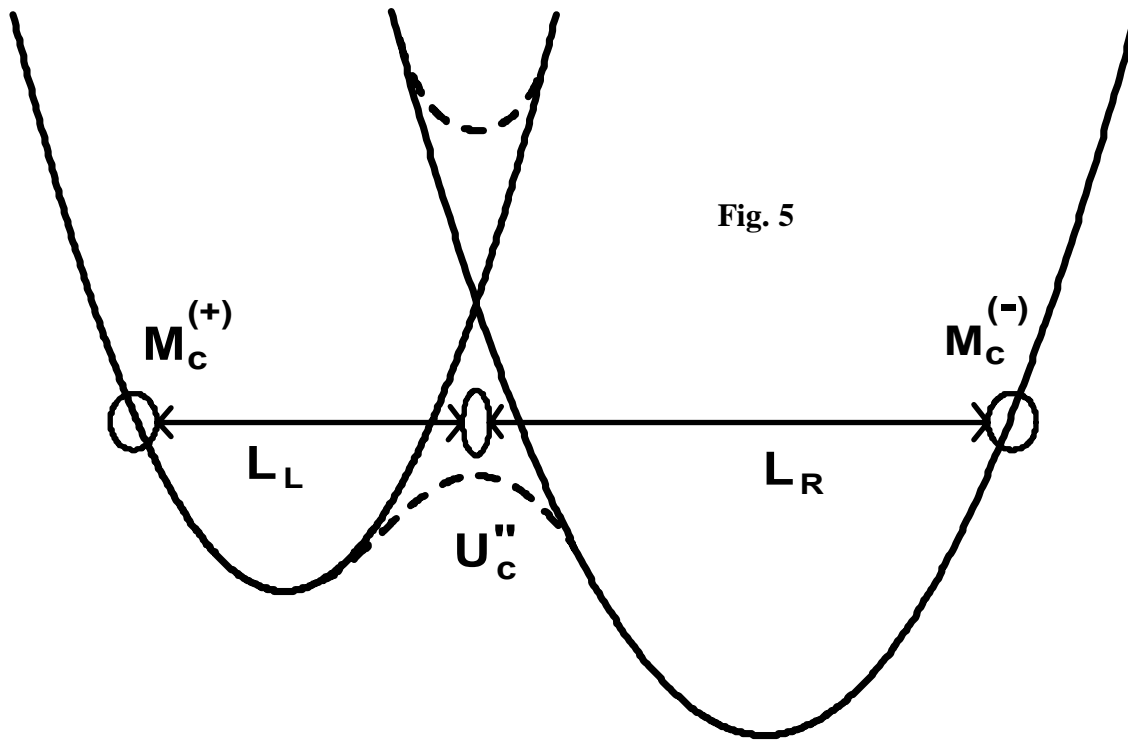


Fig. 5

$$-\frac{1}{2} \frac{d^2 \Theta_L}{dx^2} + \gamma^2 [U_L(x) - E] \Theta_L = \gamma^2 U_{12} \Theta_R,$$

$$-\frac{1}{2} \frac{d^2 \Theta_R}{dx^2} + \gamma^2 [U_R(x) - E] \Theta_R = \gamma^2 U_{12} \Theta_L.$$

$$\frac{d^4 \Theta_L}{dx^4} - 2\gamma^2 [U_L(x) + U_R(x) - 2E] \frac{d^2 \Theta_L}{dx^2} - 4\gamma^2 \frac{dU_L}{dx} \frac{d\Theta_L}{dx} + 4\gamma^4 \left[ (U_L - E)(U_R - E) - U_{12}^2 - \frac{1}{2\gamma^2} \frac{d^2 U_L}{dx^2} \right] \Theta_L = 0.$$

$$\Psi = \exp(\kappa X)\Phi$$

$$D^4\Phi + 4\kappa D^3\Phi + (6\kappa^2 - 2\alpha\gamma^2)D^2\Phi + 4\left(\kappa^3 - \alpha\gamma^2\kappa - \frac{1}{2}\gamma^2 f\right)D\Phi \quad (4)$$

$$+ [\kappa^4 - 2\alpha\gamma^2\kappa^2 - 2\gamma^2 f\kappa + \gamma^4(\alpha^2 - u_{12}^2 - f^2 X^2)]\Phi = 0,$$

$$\alpha = 2 \frac{U^\# - E}{\gamma \hbar \Omega}, \quad f = \frac{2a_0 F}{\gamma \hbar \Omega}, \quad u_{12} = \frac{2U_{12}}{\gamma \hbar \Omega},$$

$$\Psi_j^{(sc)} = (u_{12}^2 + f^2 X^2)^{-1/4} \exp\left(\int_0^X \lambda_j(x) dx\right),$$

$$j = (++ , +- , -+ , --),$$

$$\lambda_j = \lambda_j^0 + u_j, \quad \lambda_j^0 = \pm \sqrt{\gamma(\alpha \pm \sqrt{u_{12}^2 + f^2 X^2})},$$

$$\text{and } u_j = \gamma f ((\lambda_j^0)^2 - \alpha \gamma)^{-1}.$$

$$D^2 \Phi + (a_0 + a_1 X + a_2 X^2) \Phi = 0,$$

$$a_0 = \kappa^2 - \alpha \gamma^2 - \frac{\gamma^2 f}{2\kappa} (1 + \delta);$$

$$a_1 = \gamma^2 f \delta; \quad a_2 = -\gamma^2 f \kappa \delta,$$

$$\delta = \frac{\gamma^2 f}{4\kappa^3}.$$

$$D_p \left[ \pm \left( \frac{\gamma^4 f^2}{\kappa^2} \right)^{1/4} \left( X - \frac{1}{2\kappa} \right) \right], \quad p = -\frac{1}{2} + \left( \frac{\gamma^4 f^2}{\kappa^2} \right)^{-1/2} \left( a_0 - \frac{a_1^2}{4a_2} \right).$$

$$\kappa = \pm \kappa_0 \left( 1 \pm \frac{\delta^2 \kappa_0^2}{2(2\kappa_0^2 - \alpha\gamma^2)} \right);$$

$$\kappa_0 = \frac{\gamma}{\sqrt{2}} (\alpha + \sqrt{\alpha^2 - u_{12}^2})^{1/2},$$

**In the tunneling region**

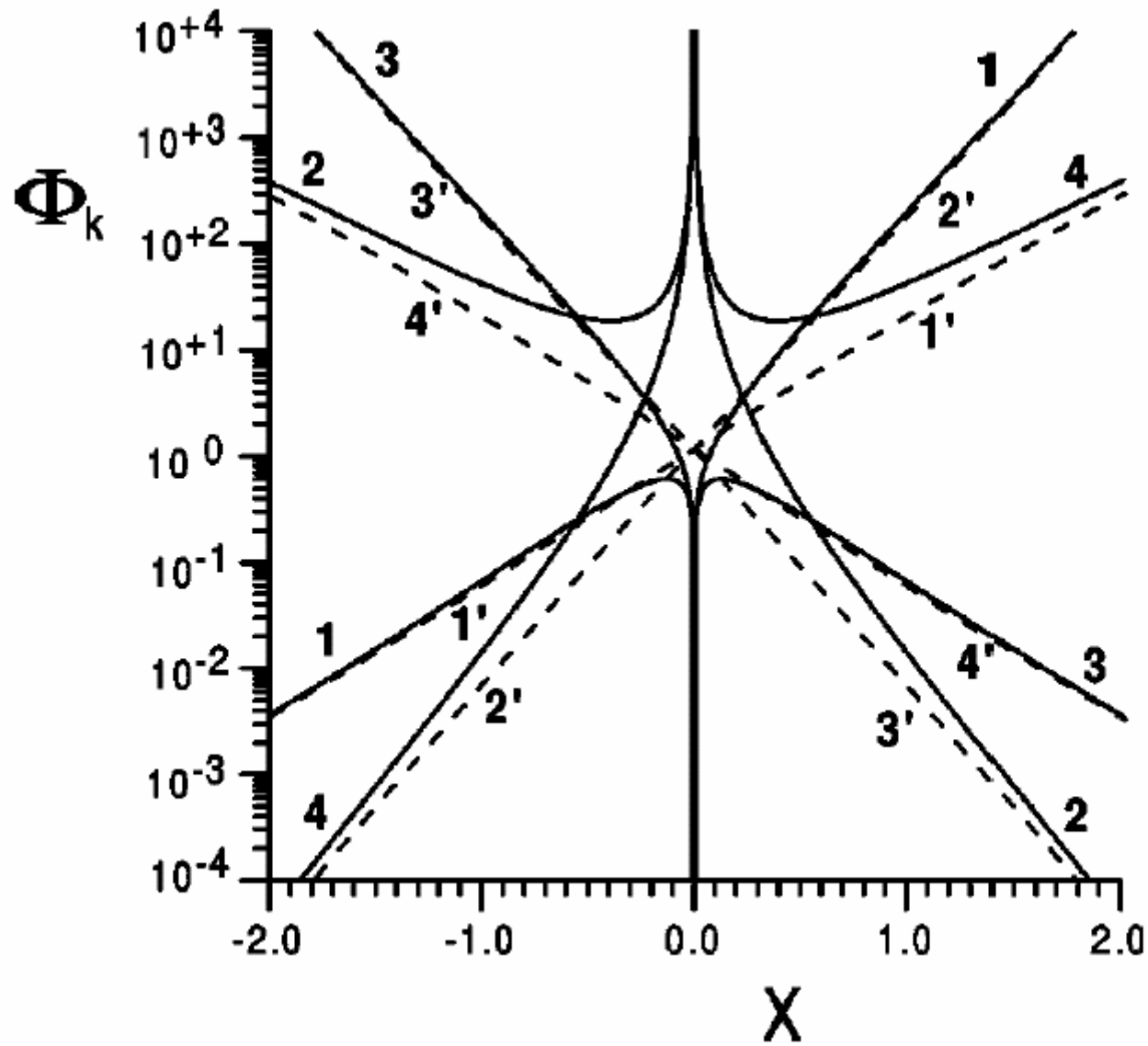


FIG. 6. The matching of the asymptotic solutions in the tunneling region for the diabatic levels crossing shown in Fig. 1(a): 1 - the function  $\Phi_L^+(X)\sqrt{2\pi}/\Gamma(1+\nu)$ ; 2- the function  $\Phi_L^-(X)$ ; 3 - the function  $\Phi_R^+(X)\sqrt{2\pi}/\Gamma(1+\nu)$ ; 4 - the function  $\Phi_R^-(X)$ ; 1' - the function  $\exp(k_0X)D_{-1-\nu}(\beta X)$ ; 2' - the function  $\exp(k_0X)D_{-1-\nu}(-\beta X)$ ; 3' - the function  $\exp(-k_0X)D_{-1-\nu}(\beta X)$ ; 4' - the function  $\exp(-k_0X)D_{-1-\nu}(-\beta X)$ .

$$k_0 = \gamma\sqrt{\alpha}$$

$$\Phi \propto \exp\left(\kappa X + \delta(\kappa X)^2 - \frac{2}{3}\delta^2(\kappa X)^3 + \dots\right).$$

**In the intermediate coupling region:**

$$\kappa_{1,2} \simeq \pm\gamma \sqrt{\frac{u_{12}}{2}} \exp(i\varphi);$$

$$\kappa_{3,4} \simeq \pm i\gamma \sqrt{\frac{u_{12}}{2}} \exp(-i\varphi),$$

$$\tan \varphi = \sqrt{\frac{u_{12} - \alpha}{u_{12} + \alpha}}.$$

$$z_1 = z_2 = 2\kappa_{\text{int}}\sqrt{\delta_{\text{int}}}\exp(-i\varphi/2)(X - (2\kappa_{\text{int}})^{-1}\exp(-i\varphi)),$$

$$z_3 = z_4 \quad (17)$$

$$= 2\kappa_{\text{int}}\sqrt{\delta_{\text{int}}}\exp(i\varphi/2)(X - (2\kappa_{\text{int}})^{-1}\exp(i\varphi)),$$

and

$$p_1 = p_2 - 1$$

$$= -1 - \frac{1}{4\delta_{\text{int}}}\exp(-i\varphi)(1 + 2\delta_{\text{int}}^2\exp(-2i\varphi)), \quad (18)$$

$$p_4 = p_3 - 1 = -1 - \frac{1}{4\delta_{\text{int}}}\exp(i\varphi)(1 + 2\delta_{\text{int}}^2\exp(2i\varphi)),$$

$$\kappa_{\text{int}} = \gamma(u_{12}/2)^{1/2}; \quad \delta_{\text{int}} = (\gamma^2 f)/(4\kappa_{\text{int}}^3).$$

$$D_p(z) \propto \exp\left[-\frac{1}{2}\int\left(z^2 - 4\left(p + \frac{1}{2}\right)\right)^{1/2} dz\right].$$

$$\Phi_0 \propto \exp\left(-i\int\sqrt{a_0 + a_1X + a_2X^2} dx\right)$$

$$\Psi_j^\pm = \exp(\kappa X)D_p(\pm z_j(X)), \quad (22)$$

and

$$\begin{aligned} \Psi_1^+, \Psi_4^+ &\propto \exp(F_1(X)), & \Psi_2^-, \Psi_3^- &\propto \exp(-F_1(X)), \\ \Psi_1^-, \Psi_3^- &\propto \exp(iF_2(X)), & \Psi_2^+, \Psi_4^- &\propto \exp(-iF_2(X)), \end{aligned} \quad (23)$$

$$\begin{aligned}
F_{1,2}(X) &= \gamma \sqrt{u_{12} \pm \alpha} (1 + \delta_{\text{int}}) X - \kappa_{\text{int}}^2 \delta_{\text{int}}^2 \exp(-2i\varphi) X^2 \\
&+ \frac{\gamma f^2}{12 u_{12} \sqrt{u_{12} \pm \alpha}} \left( 1 \pm \frac{\alpha}{u_{12}} - \delta_{\text{int}} \right) X^3. \quad (24)
\end{aligned}$$

$$\begin{aligned}
\Psi_1^+ + \Psi_4^+ &\longrightarrow \Psi_{++}^{SC}; & \Psi_2^- + \Psi_3^- &\longrightarrow \Psi_{+-}^{SC}; \\
\Psi_1^- + \Psi_3^+ &\longrightarrow \Psi_{-+}^{SC}; & \Psi_2^+ + \Psi_4^- &\longrightarrow \Psi_{--}^{SC},
\end{aligned}$$



$$q = q_1 + iq_2; \quad q_{1,2} = \frac{\gamma u_{12} \sqrt{u_{12} \pm \alpha}}{4f};$$

$$\chi = \chi_1 + i\chi_2; \quad 2\chi_1 = q_1 - \left(q_1 - \frac{1}{2}\right) \ln|q| + \varphi q_2$$

$$2\chi_2 = q_2 - q_2 \ln|q| - \varphi \left(q_1 - \frac{1}{2}\right),$$

**These relations provide asymptotically smooth matching of the semiclassical solutions with the Weber functions when:**

$\kappa$  is of the order of  $\gamma \gg 1$

**and with the Airy solutions when:**  $\kappa \approx \sqrt{\gamma}$ .